Supporting Information for:

Copper(II) complexes with tridentate Schiff base-like ligands: solid state and solution structures and anticancer activity

Katja Dankhoff[+],[a] Madeleine Gold[+],[b] Luisa Kober,[b] Florian Schmitt,[b] Lena Pfeifer,[a] Andreas Dürrmann,[a] Hana Kostrhunova,[c] Matthias Rothemund,[b] Viktor Brabec,[c] Rainer Schobert,*[b] and Birgit Weber*[a]

[a] Department of Chemistry, Inorganic Chemistry IV, Universität Bayreuth, Universitätsstr. 30, 95447 Bayreuth, Germany, e-mail: weber@uni-bayreuth.de

[b] Department of Chemistry, Organic Chemistry I, Universität Bayreuth, Universitätsstr. 30, 95447 Bayreuth, Germany

[c] Czech Academy of Sciences, Institute of Biophysics, Kralovopolska 135, CZ-61265 Czech Republic

[+] These authors contributed equally to this work.

Table S1. Crystallographic data of the complexes discussed in this work.

	4	**5**	**7**	**8**	**9**
CCDC	1566628	1566629	1566630	1566631	1566632
formula	$[(\mu_2\text{–Br})_2(\text{CuL1})_2]$	$[(\mu_2\text{–Br})_2(\text{CuL2})_2]$	$[(\mu_2\text{–Br})(\text{CuL4})]_n$	$[(\mu_2\text{–Br})_2(\text{CuL5})_2]$	$[(\mu_2\text{–Br})_2(\text{CuL6})_2]$
sum formula	$C_{26}H_{30}Br_2Cu_2N_4O_6$	$C_{24}H_{26}Br_2Cu_2N_4O_4$	$C_{12}H_{12}BrCuN_3O_2$	$C_{36}H_{34}Br_2Cu_2N_4O_6$	$C_{24}H_{26}Br_2Cu_2N_4O_6$
M/ g mol^{-1}	781.44	721.39	373.70	905.57	753.38
crystal system	triclinic	triclinic	monoclinic	monoclinic	triclinic
space group	P–1	P–1	$P2_1/c$	$P2_1/n$	P–1
crystal description	blue green block	blue block	green plate	green block	blue green prism
a/ Å	7.7302(4)	7.9933(7)	7.6905(4)	10.5383(6)	8.0566(4)
b/ Å	9.2879(5)	9.2785(11)	24.3476(14)	9.5476(5)	8.4259(4)
c/ Å	10.2517(5)	9.4396(10)	7.7833(4)	17.4636(12)	11.1094(5)
α/ °	94.782(4)	90.031(9)	90	90	75.675(4)
β/ °	94.310(4)	98.575(7)	113.207(4)	100.791(5)	86.846(4)
γ/ °	108.849(4)	111.440(8)	90	90	68.045(4)
V/ Å^3	690.07(6)	643.21(12)	1339.46(13)	1726.04(18)	677.12(6)
Z	1	1	4	2	1
ρ_{calcd}/ g cm^{-3}	1.880	1.862	1.853	1.742	1.848
μ/ mm^{-1}	4.485	4.798	4.614	3.600	4.567
crystal size/ mm	0.090×0.070×0.065	0.110×0.105×0.097	0.110×0.102×0.093	0.104×0.097×0.093	0.099×0.084×0.075
F(000)	390	358	740	908	374
T/ K	133(2)	133(2)	133(2)	133(2)	133(2)
λ/ Å	Mo-K_α 0.71073	Mo-K_α 0.71073	Mo-K_α 0.71073	Mo-K_α 0.71073	Mo-K_α 0.71073
Θ range/ °	2.00–28.50	2.2–28.6	1.68–28.67	2.11–28.47	1.9–28.4
Reflns. collected	3242	7822	3151	4145	3198
Indep. reflns.(R_{int})	2709 (0.0317)	3021 (0.1611)	2226 (0.0608)	2693 (0.1860)	2677 (0.0299)
Parameters	181	163	172	226	172
$R1$ (all data)	0.0266 (0.0361)	0.0814 (0.1116)	0.0404 (0.0654)	0.0733 (0.1115)	0.0241 (0.0332)
$wR2$	0.0628	0.2878	0.1099	0.2261	0.0560
GooF	0.985	1.064	0.960	1.011	0.997

Table S1. (continued)

	12	**15**	**17**	**18**
CCDC	1915615	1915614	1915617	1915616
formula	[CuL9Br]	[CuL12Br]	[CuL14Br]	[CuL15Br]
sum formula	$C_{14}H_{16}BrClCuN_2O_4$	$C_{13}H_{14}BrCuN_3O_2$	$C_{15}H_{19}BrCuN_2O_4$	$C_{13}H_{14}BrCuN_3O_2$
M/ g mol^{-1}	455.19	387.72	434.77	387.72
crystal system	triclinic	triclinic	monoclinic	triclinic
space group	P–1	P–1	$P2_1/a$	P–1
crystal description	green cube	green plate	green plate	green plate
a/ Å	8.0351(3)	7.8986(4)	7.9002(3)	7.5494(2)
b/ Å	9.6830(3)	8.2689(3)	18.0037(6)	8.2358(3)
c/ Å	11.4547(4)	11.3892(4)	11.3870(5)	12.3671(4)
α/ °	98.869(3)	85.890(3)	90	107.000(3)
β/ °	102.321(3)	78.823(3)	94.962(4)	96.398(3)
γ/ °	104.864(3)	81.476(3)	90	102.191(3)
V/ Å^3	820.70(5)	720.98(5)	1613.54(11)	706.30(4)
Z	2	2	4	2
ρ_{calcd}/ g cm^{-3}	1.842	1.786	1.790	1.823
μ/ mm^{-1}	3.947	4.289	3.851	4.378
crystal size/ mm	0.095×0.076×0.065	0.119×0.117×0.098	0.079×0.052×0.037	0.085×0.045×0.032
F(000)	454	386	876	386
T/ K	133(2)	133(2)	133(2)	133(2)
λ/ Å	Mo-K_α 0.71073	Mo-K_α 0.71073	Mo-K_α 0.71073	Mo-K_α 0.71073
Θrange/ °	1.9–28.5	1.8–29.1	1.6–28.4	1.8–28.5
Reflns. collected	12083	8912	12531	10623
Indep. reflns.(R_{int})	3966 (0.030)	3350 (0.028)	3900 (0.058)	3406 (0.027)
Parameters	208	181	208	181
R1 (all data)	0.0368 (0.0504)	0.0296 (0.0431)	0.0430 (0.0642)	0.0272 (0.0400)
wR2	0.0995	0.0741	0.1137	0.0659
GooF	1.04	1.034	1.04	1.05

Table S2. Selected bond lengths/Å and angles/° of the complexes discussed in this work.

	Cu–N_{py}	Cu–N	Cu–O	Cu–X	Cu–X–Cu	X–Cu–X
4	2.0126(19)	1.928(2)	1.9363(18)	2.4316(4) 2.8919(4)	91.15(1)	88.85(1)
5	1.993(7)	1.924(8)	1.926(6)	2.4419(14) 2.9264(15)	91.16(4)	88.84(4)
7	1.995(3)	1.949(3)	1.951(3)	2.4153(6) 2.8131(6)	95.92(2)	96.08(2)
8	1.994(6)	1.945(5)	1.918(4)	2.4330(12) 2.9152(12)	86.70(4)	93.30(3)
9	2.0001(17)	1.9316(17)	1.9256(17)	2.4281(3) 2.9752(4)	91.17(1)	88.83(1)
12	1.995(3)	1.930(3)	1.923(3)	2.3787(5)	/	/
15	2.026(2)	1.976(2)	1.9730(18)	2.4174(4)	/	/
17	1.990(3)	1.936(3)	1.940(2)	2.3770(6)	/	/
18	2.005(2)	1.928(3)	1.9481(16)	2.3588(4)	/	/

Figure S1. Structures of **5**(top left), **8** (top middle), **9** (top right), **12** (bottom left), **15** (bottom middle), and **18** (bottom right). Ellipsoids were drawn at 50 % probability level. Hydrogen atoms were omitted for clarity.

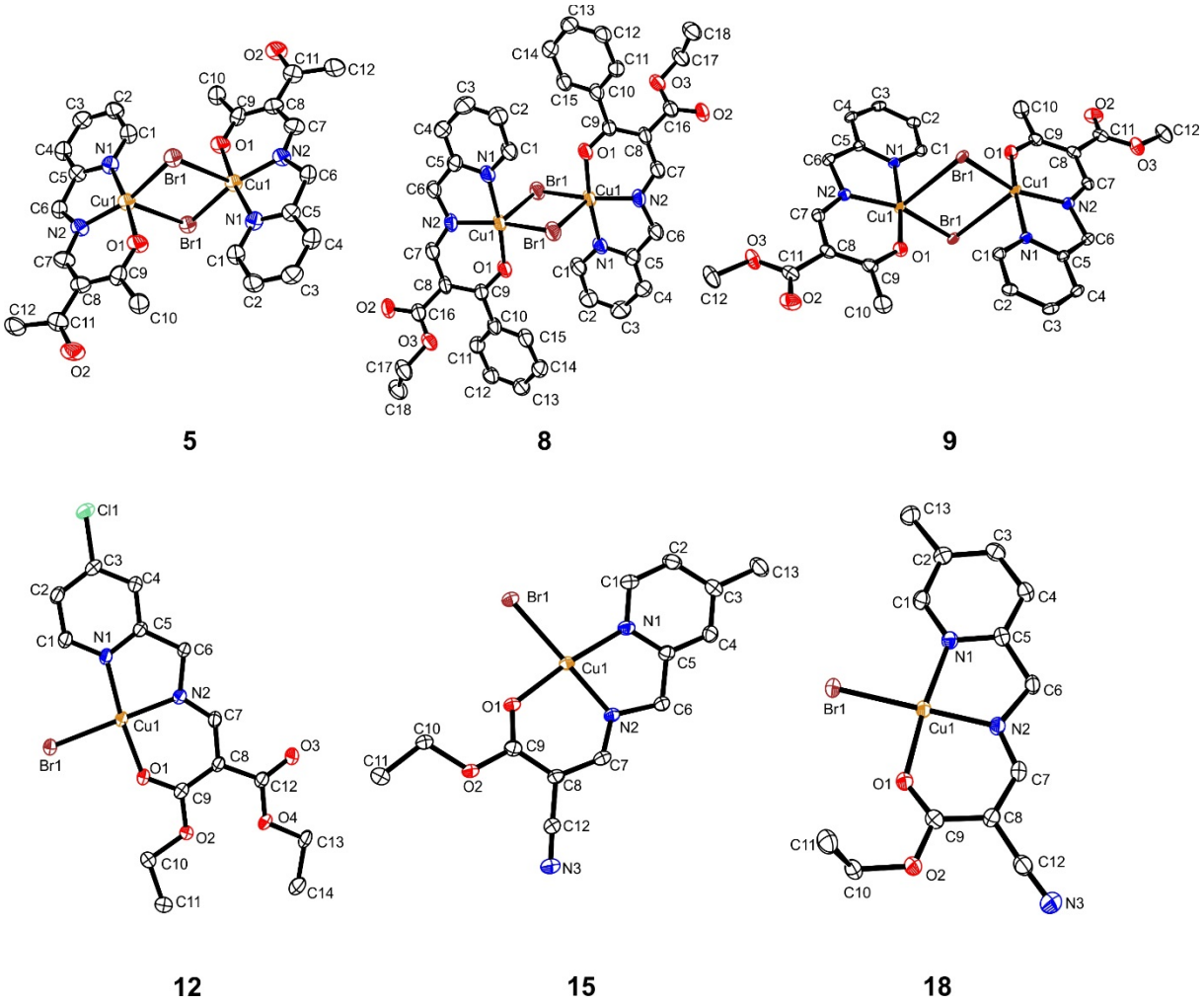

Table S3. Summary of the C–H···π / X–Y···π interactions of the complexes presented in this work.

		C_g	H···C_g/Å Y···C_g/Å	X–H···C_g/° X–Y···C_g/°	X···C_g/Å
5	C12–H12A	Cu1–O1–C9–C8–C7–N2[a]	2.83	141	3.644(11)
7	C6–H6A	Cu1–O1–C9–C8–C7–N2[b]	2.66	141	3.485(4)
	C10–H10B	N1–C1–C2–C3–C4–C5[c]	2.81	141	3.634(5)
12	C3–Cl1	Cu1–N1–C5–C6–N2[d]	3.3478(14)	84.40(11)	3.614(3)
17	C10–H10A	N1–C1–C2–C3–C4–C5[e]	2.98	132	3.709(4)
	Cu1–Br1	Cu1–N1–C5–C6–N2[f]	3.3662(14)	83.37(3)	3.8900(14)
	Cu1–Br1	N1–C1–C2–C3–C4–C5[f]	3.8784(15)	118.56(3)	5.4320(15)

a: −3−x, −y, −z; b: x, 3/2−y, 1/2+z; c: x, 3/2−y, −1/2+z; d: 1−x, −y, 2−z; e: −1/2+x, 1/2−y, z; f: 1/2+x, 1/2−y, z.

Table S4. Selected distances and angles of the π– π and M– π interactions of the complexes presented in this work. C_g(I) is the centroid of the ring number I, α is the dihedral angle between the rings, β is the angle between the vector C_g(I) → C_g(J) and the normal to ring I, γ is the angle between the vector C_g(I) → C_g(J) and the normal to ring J.

	C_g(I)	C_g(J)	C_g–C_g/Å	α/°	β/°	γ/°
4	Cu1–O1–C9–C8–C7–N2	N1–C1–C2–C3–C4–C5[a]	3.9305(14)	2.29(11)	25.5	24.0
9	N1–C1–C2–C3–C4–C5	Cu1[b]	3.982	0	29.86	0
12	Cu1–N1–C5–C6–N2	Cu1–O1–C9–C8–C7–N2[b]	3.3580(16)	2.53(12)	9.6	9.8
	N1–C1–C2–C3–C4–C5	N1–C1–C2–C3–C4–C5[c]	3.4951(18)	0.02(15)	17.4	17.4
	Cu1–N1–C5–C6–N2	Cu1[b]	3.544	0	22.30	0
	Cu1–O1–C9–C8–C7–N2	Cu1[b]	3.707	0	28.89	0
15	Cu1–N1–C5–C6–N2	Cu1–O1–C9–C8–C7–N2[d]	3.2977(14)	3.99(10)	11.6	11.9
	Cu1–N1–C5–C6–N2	N1–C1–C2–C3–C4–C5[a]	3.6338(14)	0.81(12)	19.5	18.7
	Cu1–N1–C5–C6–N2	Cu1[d]	3.635	0	30.33	0
	Cu1–O1–C9–C8–C7–N2	Cu1[d]	3.423	0	20.86	0
	N1–C1–C2–C3–C4–C5	Cu1[a]	3.570	0	16.69	0
17	Cu1–N1–C5–C6–N2	Cu1–O1–C9–C8–C7–N2[e]	3.5852(18)	4.02(14)	21.8	18.6
	Cu1–N1–C5–C6–N2	Cu1[f]	3.890	0	32.59	0
	Cu1–O1–C9–C8–C7–N2	Cu1[f]	3.444	0	16.48	0
18	Cu1–N1–C5–C6–N2	Cu1–N1–C5–C6–N2[g]	3.5980(14)	0.02(11)	20.0	20.0
	Cu1–N1–C5–C6–N2	Cu1–O1–C9–C8–C7–N2[h]	3.4963(13)	1.40(10)	22.6	23.6
	Cu1–N1–C5–C6–N2	N1–C1–C2–C3–C4–C5[g]	3.6748(13)	3.91(11)	22.6	22.3
	Cu1–O1–C9–C8–C7–N2	N1–C1–C2–C3–C4–C5[g]	3.5589(13)	2.74(10)	17.7	18.0
	Cu1–N1–C5–C6–N2	Cu1[h]	3.650	0	28.30	0
	Cu1–N1–C5–C6–N2	Cu1[g]	3.907	0	30.19	0
	Cu1–O1–C9–C8–C7–N2	Cu1[h]	3.322	0	14.07	0
	N1–C1–C2–C3–C4–C5	Cu1[g]	3.548	0	21.11	0

a: 1−x, 1−y, −z; b: 1−x, 1−y, 2−z; c: 1−x, −y, 2−z; d: 1−x, −y, −z; e: 1/2+x, 1/2−y, z; f: −1/2+x, 1/2−y, z; g: 2−x, −y, 1−z; h: 1−x, −y, 1−z.

Table S5. Hydrogen bonds and angles of the complexes presented in this work.

	Donor	Acceptor	D–H/Å	H···A/Å	D···A/Å	D–H···A/°
4	C3–H3	Br1[a]	0.95	2.82	3.606(3)	140
	C6–H6B	Br1[b]	0.99	2.77	3.652(3)	149
5	C2–H2	O2[c]	0.95	2.48	3.203(12)	133
	C6–H6A	Br1[d]	0.99	2.83	3.730(9)	151
	C6–H6B	O2[e]	0.99	2.56	3.378(11)	140
7	C6–H6B	Br1[f]	0.99	2.88	3.766(4)	149
	C7–H7	Br1[g]	0.95	2.84	3.744(4)	159
8	C7–H7	O2[h]	0.95	2.39	3.318(9)	164
9	C3–H3	Br1[i]	0.95	2.90	3.602(2)	132
	C6–H6B	Br1[j]	0.99	2.92	3.829(2)	153
12	C2–H2	Br1[k]	0.95	2.91	3.842(3)	167
	C4–H4	O3[l]	0.95	2.30	3.142(4)	148
15	C6–H6A	Br1[m]	0.99	2.88	3.747(3)	147
17	C4–H4	O3[o]	0.95	2.42	3.370(5)	173
18	C7–H7	Br1[a]	0.95	2.85	3.622(2)	139
	C13–H13C	Br1[p]	0.98	2.91	3.832(3)	157

a: x, −1+y, z; b: 1−x, 1−y, −z; c: 1+x, 1+y, 1+z; d: −3−x, −y, 1−z; e: −3−x, −y, −z; f: 1+x, 3/2−y, 1/2+z; g: 1+x, y, 1+z; h: 2−x, −y, 1−z; i: −1+x, 1+y, z; j: 1−x, 1−y, 2−z; k: −x, −y, 2−z; l: 2−x, 1−y, 2−z; m: 1+x, y, z; o: −1/2−x, 1/2+y, −z; p: 2−x, 1−y, 1−z.

Figure S2. Powder X-ray diffraction patterns and calculated pattern of **4**, **5**, **7**, **8**, and **9**. Calculated patterns were obtained at 133 K, measured at room temperature.

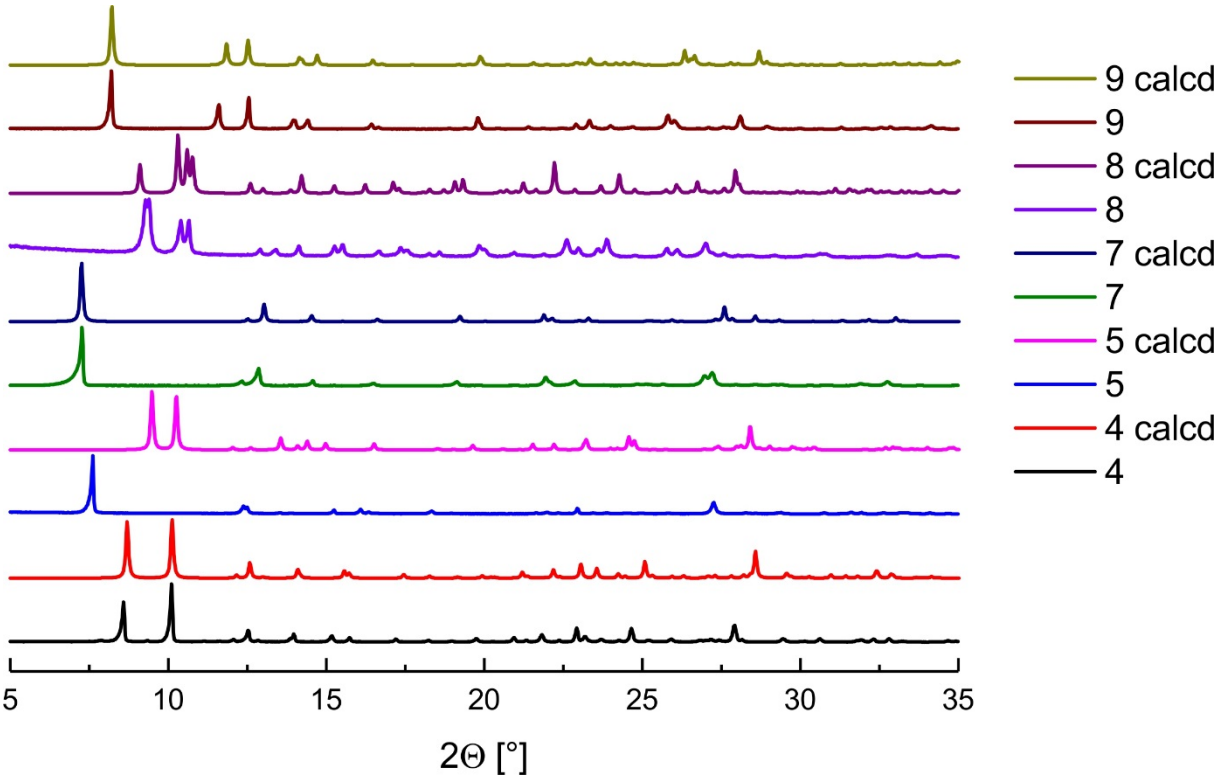

Figure S3. Powder X-ray diffraction patterns and calculated patterns of **12**, **15**, **17**, and **18**. Calculated patterns were obtained at 133 K, measured at room temperature.

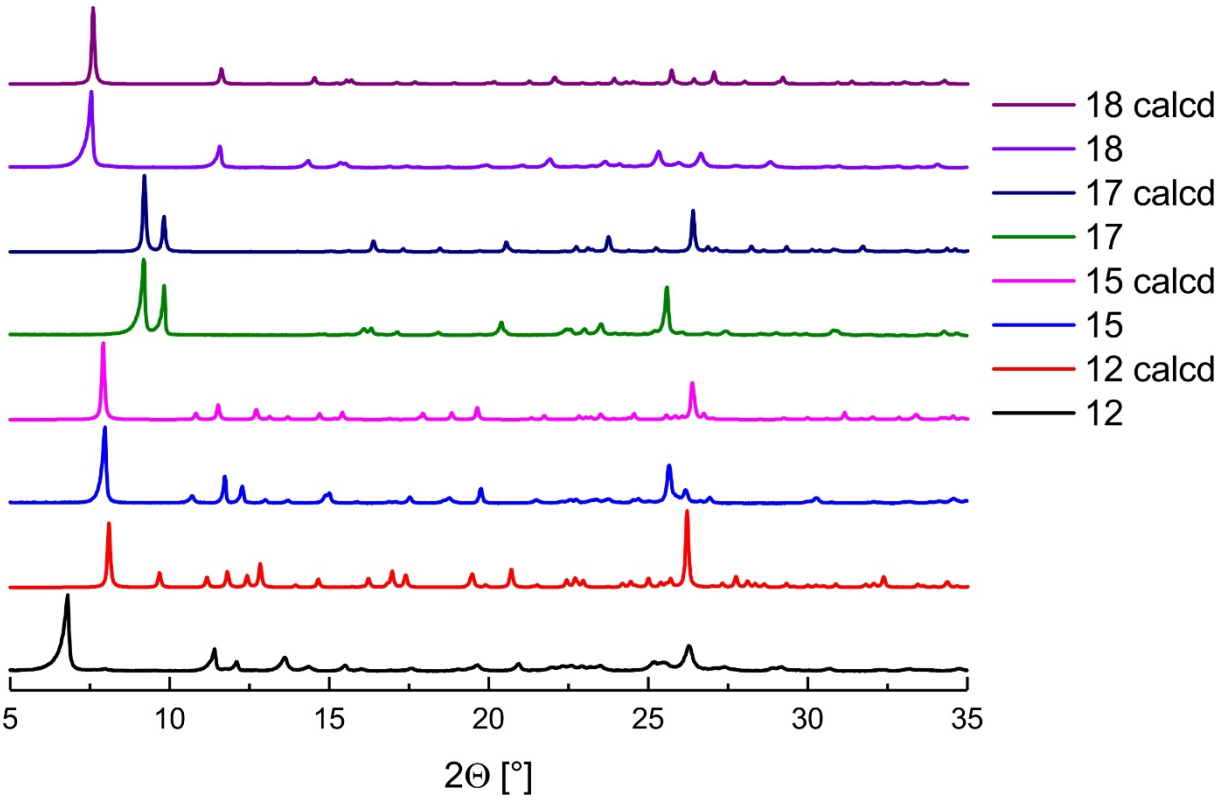

Figure S4. $\chi_M T$ vs. T plots of compounds **4**, **5**, **6**, **7**, **8**, and **9**.

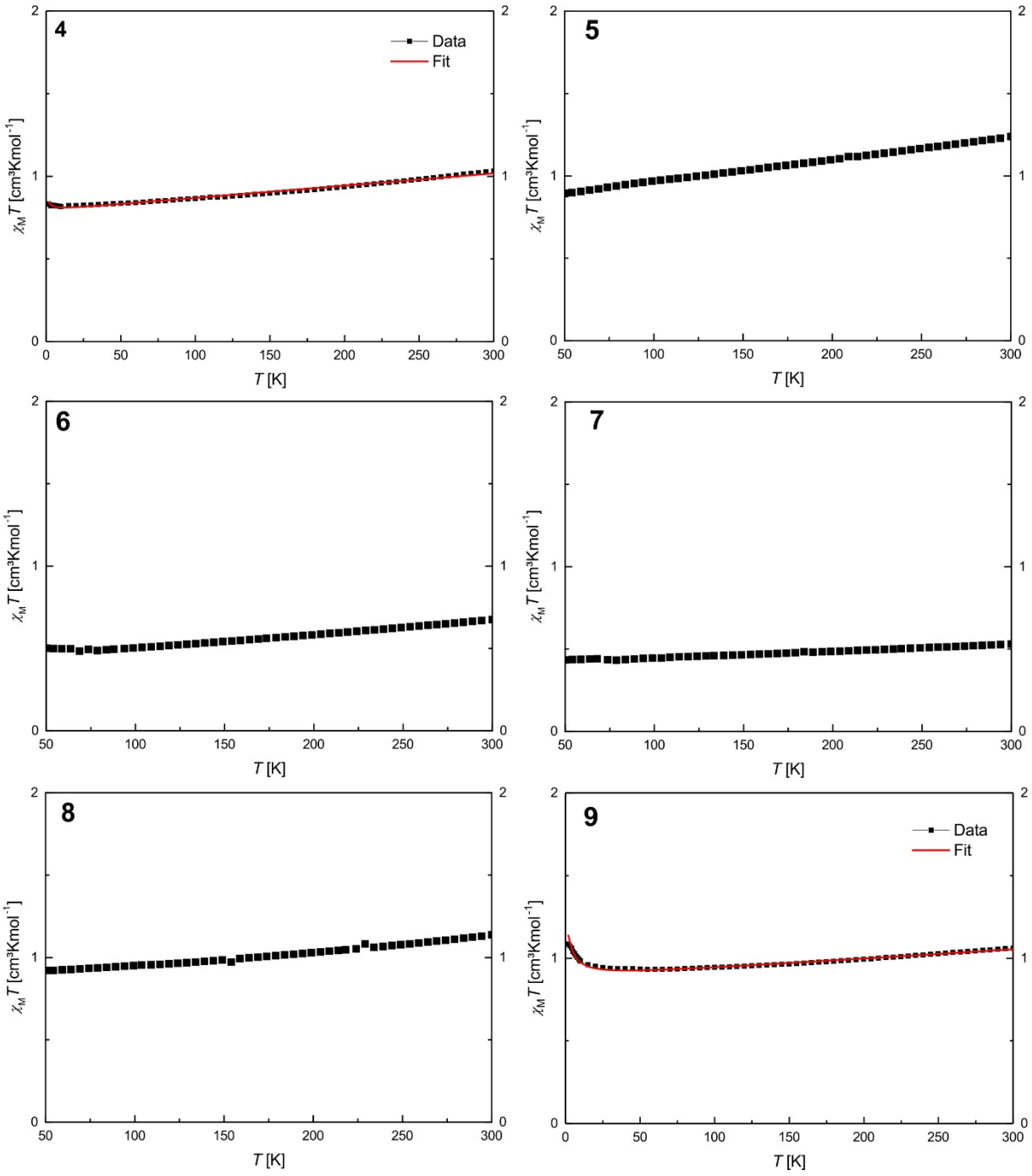

Figure S5. $\chi_M T$ vs. T plots of compounds **10**, **11**, **12**, **13**, **14**, and **15**.

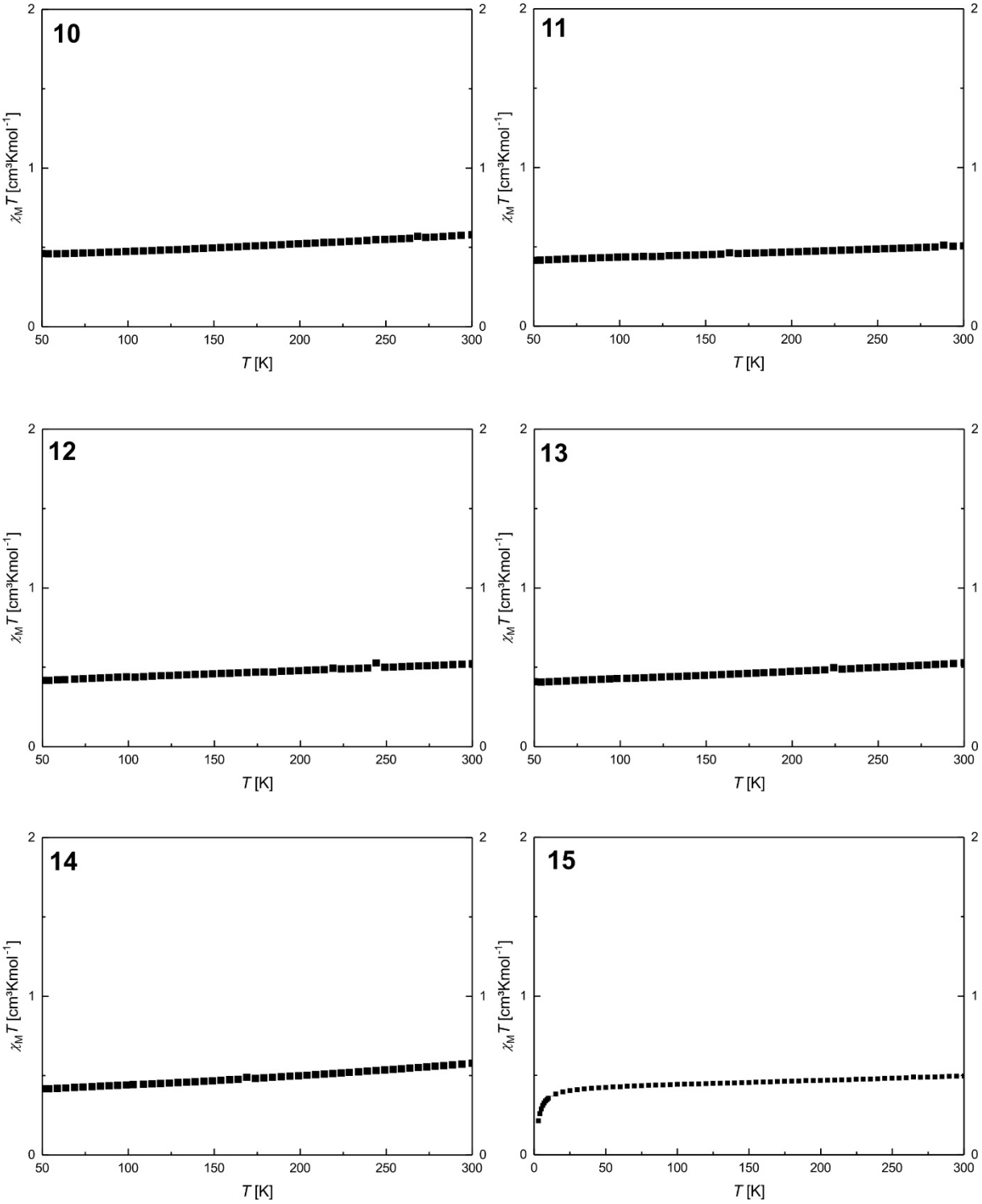

Figure S6. $\chi_M T$ vs. T plots of compounds **16**, **17**, and **18**.

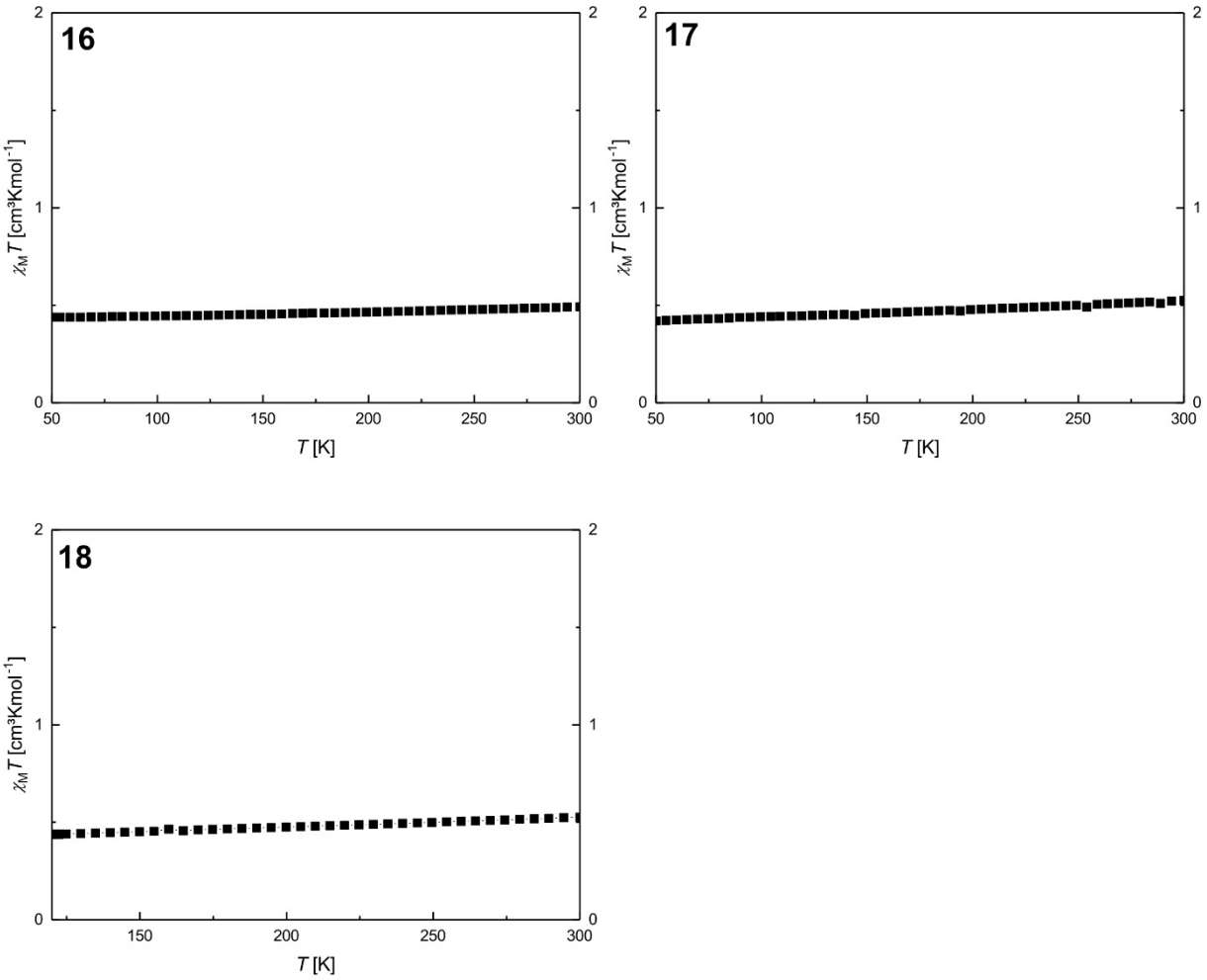

Table S6. Data of the magnetic measurements with μ_{eff} at 300 K, $\chi_M T$ at 300 K, 50 K, and, if measured, 2 K, and, if determined, the coupling constant J, g, and TIP.

	μ_{eff} [μ_B] (300 K)	$\chi_M T$ [$cm^3K^{-1}mol^{-1}$] (300 K)	$\chi_M T$ [$cm^3K^{-1}mol^{-1}$] (50 K)	$\chi_M T$ [$cm^3K^{-1}mol^{-1}$] (2 K)	J [cm^{-1}]	g	TIP [cm^3mol^{-1}]
4	2.88	1.04	0.84	0.83	0.38(5)	2.057(3)	$7.45(11)\cdot10^{-4}$
5	3.15	1.24	0.89				
6	2.33	0.68	0.50				
7	2.06	0.53	0.43				
8	3.02	1.14	0.92				
9	2.90	1.05	0.93	1.09	3.38(19)	2.163(4)	$5.79(17)\cdot10^{-4}$
10	2.16	0.58	0.46				
11	2.01	0.51	0.42				
12	2.05	0.52	0.42				
13	2.06	0.53	0.41				
14	2.15	0.58	0.42				
15	1.99	0.50	0.42	0.21			
16	1.99	0.49	0.44				
17	2.05	0.53	0.42				
18	2.05	0.53	0.44 (120 K)*				

*due to technical difficulties this complex was only measured down to 120 K.

Figure S7. UV-Vis spectra of **1**–**6** (**1** in H_2O, **2**–**6** in DMSO) at the indicated time points.

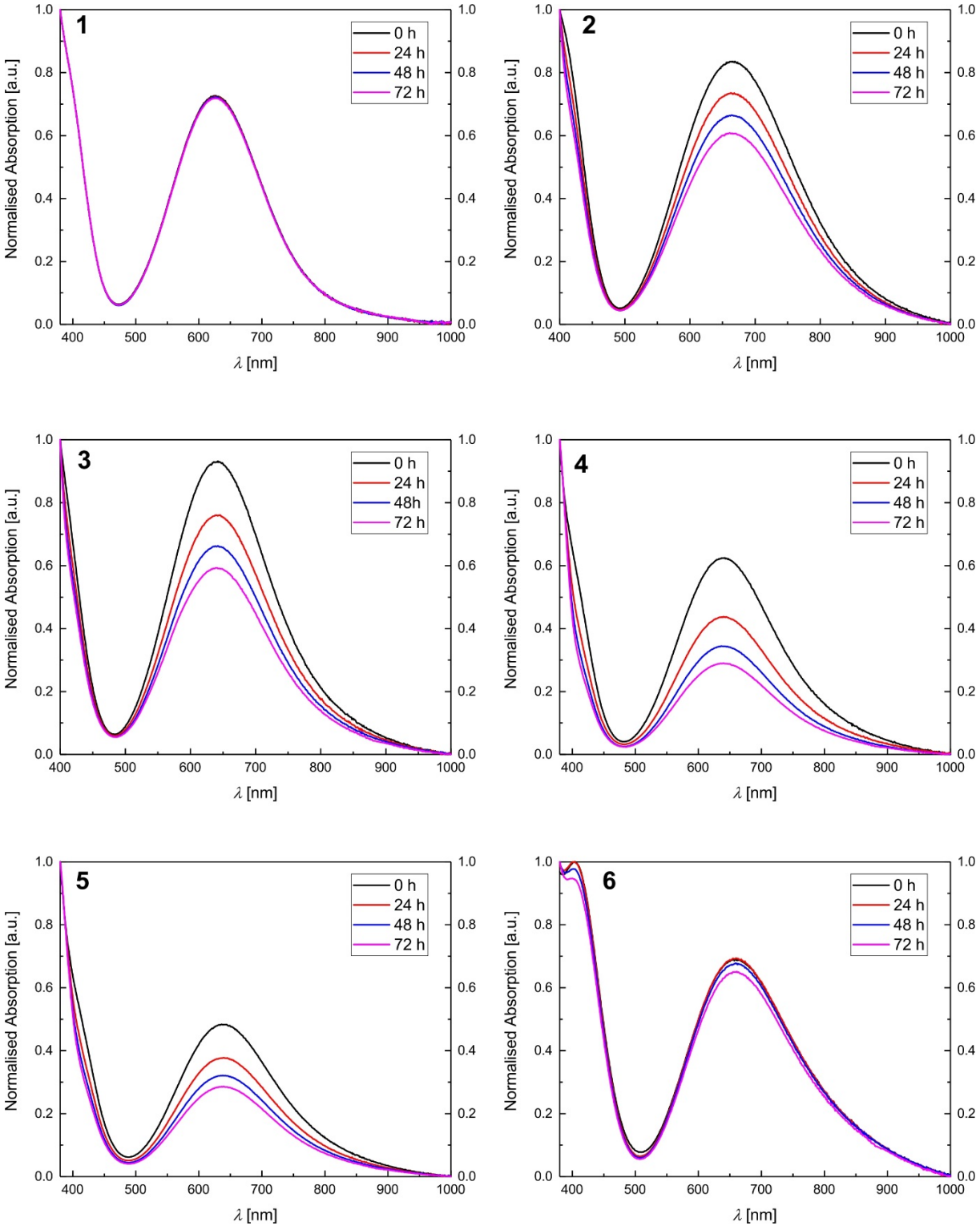

Figure S8. UV-Vis spectra of **7–12** (DMSO) at the indicated time points.

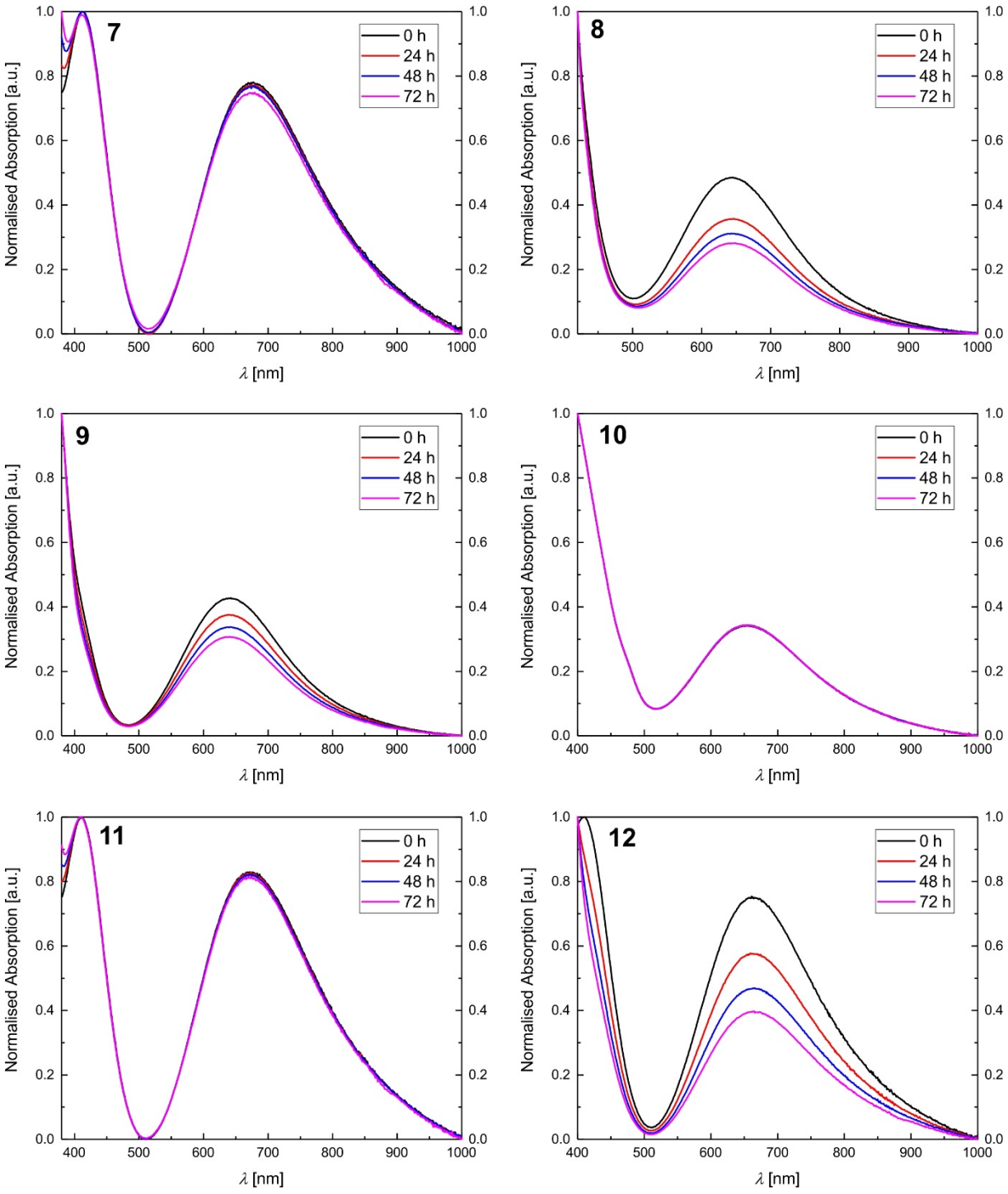

Figure S9. UV-Vis spectra of **13–18** (DMSO) at the indicated time points.

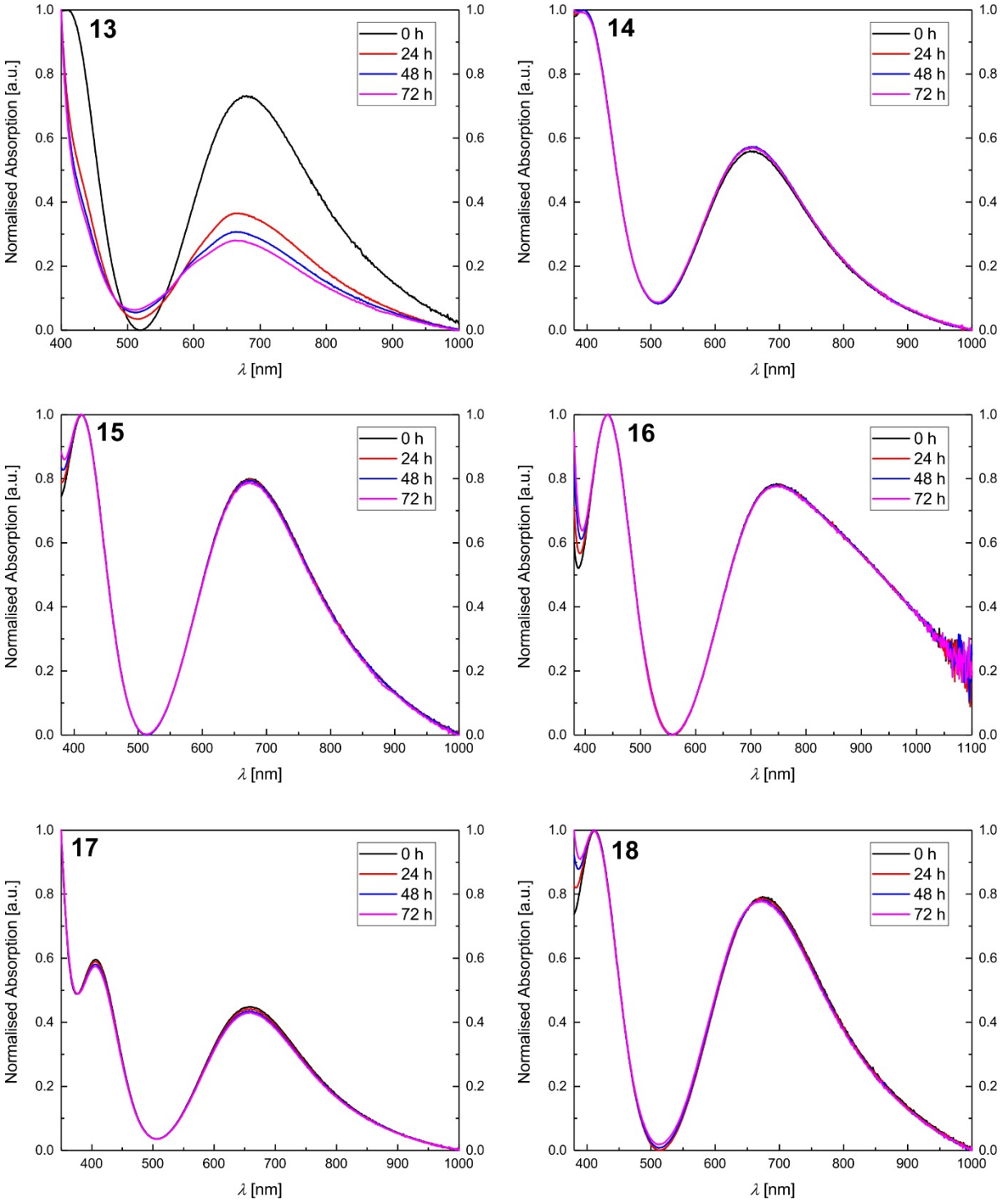

Figure S10. Cyclic voltammograms (MeCN, 0.1 M NBu_4PF_6, vs. $Ag/AgNO_3$, 50 mV/s) of **1**–**6**.

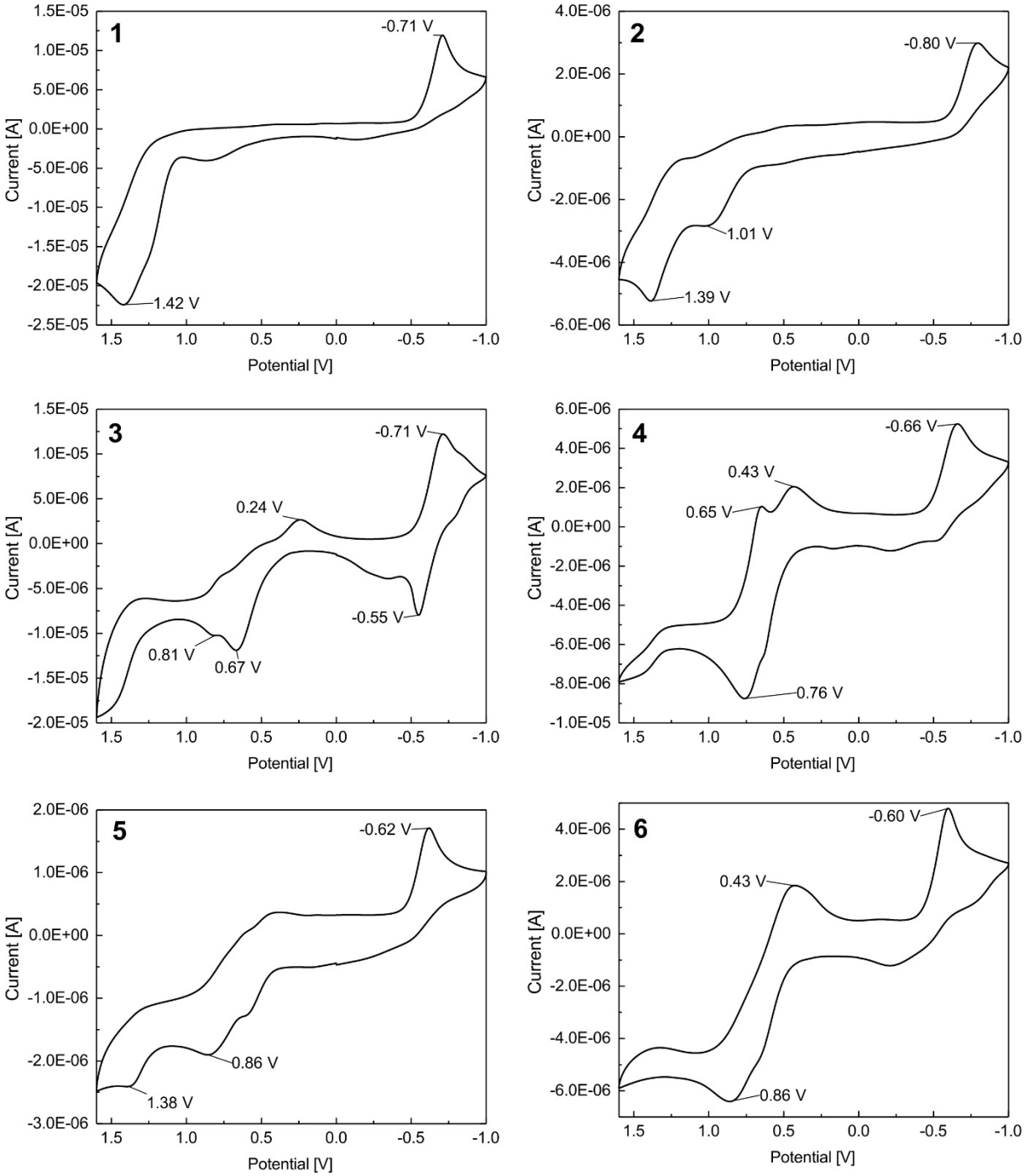

Figure S11. Cyclic voltammograms (MeCN, 0.1 M NBu_4PF_6, vs. $Ag/AgNO_3$, 50 mV/s) of **7**–**12**.

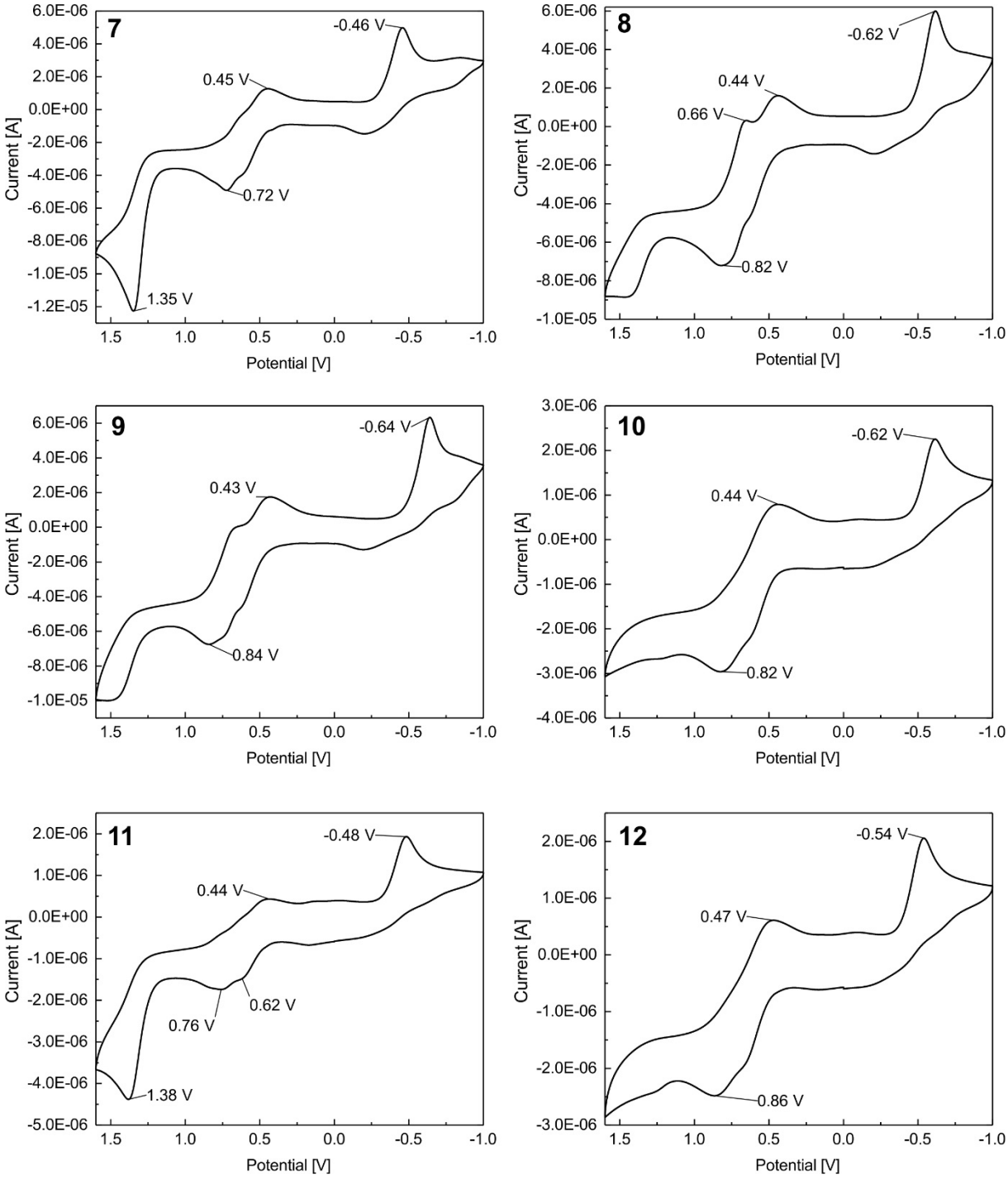

Figure S12. Cyclic voltammograms (MeCN, 0.1 M NBu_4PF_6, vs. $Ag/AgNO_3$, 50 mV/s) of **13**–**18**.

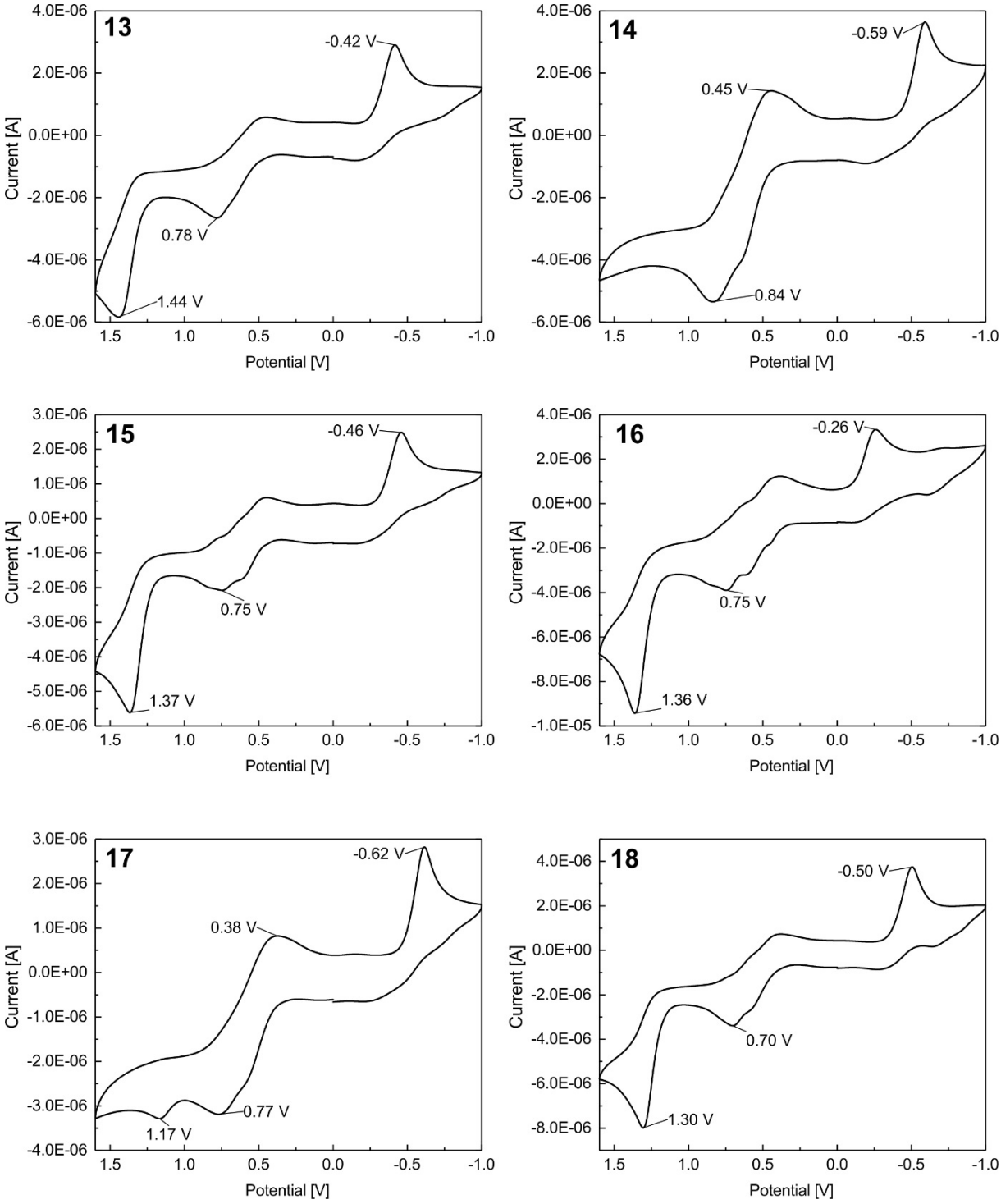

Figure S13. UV-Vis spectra of **3**, **8**, and **11** in PBS.

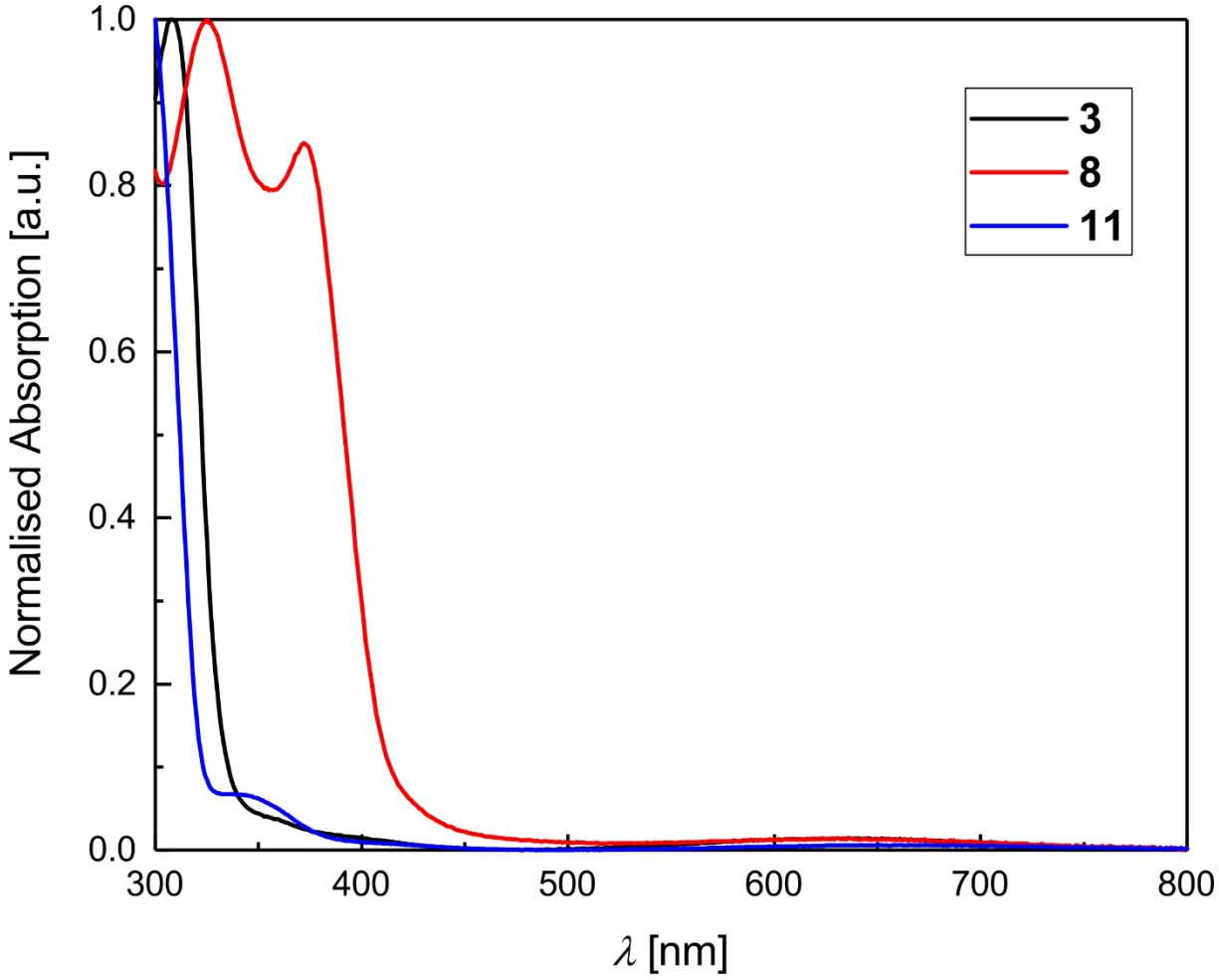

Figure S14. UV-Vis spectra of compounds **1**, **10**, and **14** (100 µM) in PBS at 37 °C at the indicated time points.

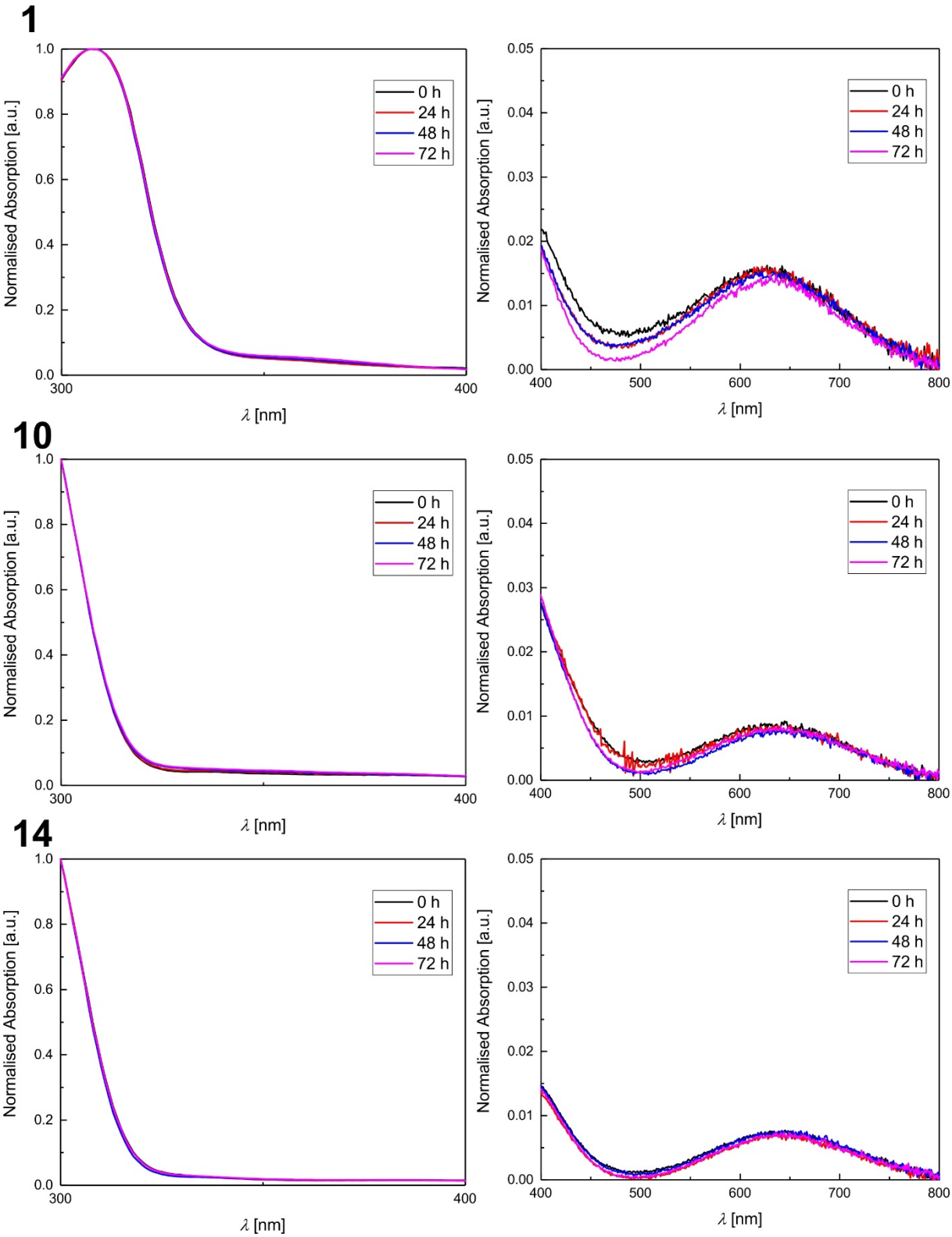

Figure S15. Relative ethidium bromide–DNA adduct fluorescence after pre-incubation with vehicle (0 µM) of **1**, **10**, **14**, and $CuSO_4$ (25, 50, 75, 100 µM) for 2 h. A decreased fluorescence indicates an interaction between DNA and test compound which prevents the intercalation of ethidium bromide molecules between the double-stranded SS-DNA. Values ± SD derived from at least three independent experiments with controls set to 100 %.

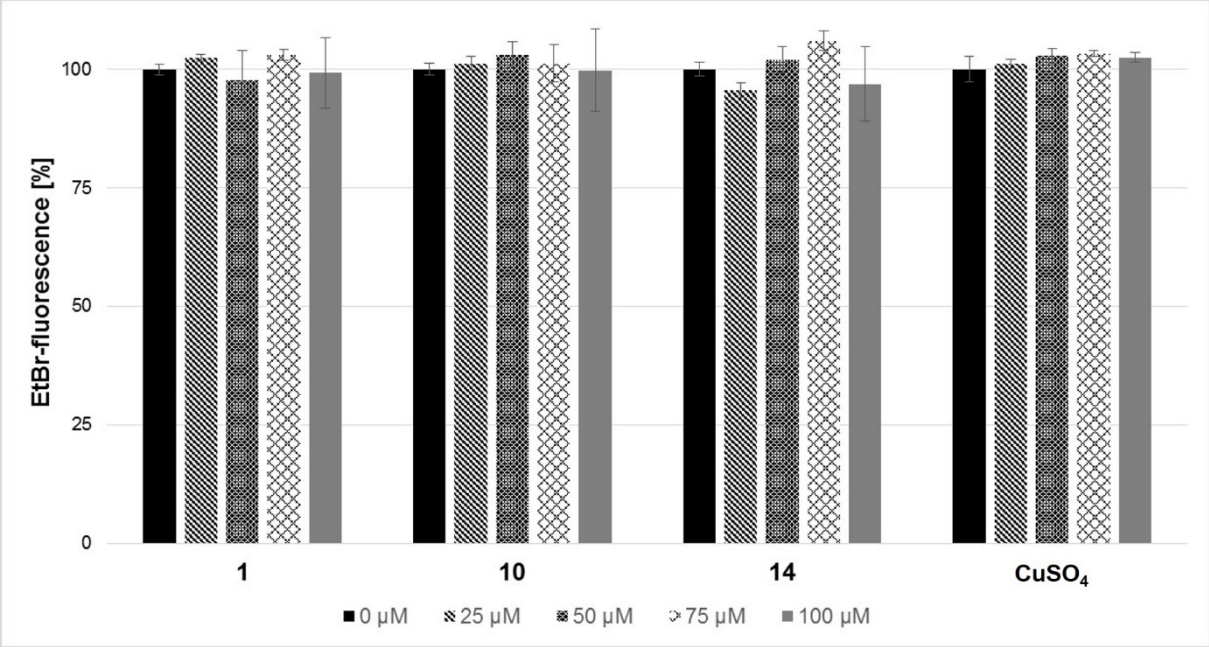

Figure S16. Electrophoretic mobility shift assay (EMSA) with circular pBR322 DNA. DNA was incubated with cis-platin (CDDP, top left), **1** (top right), **10** (bottom left), or **14** (bottom right) (0, 5, 10, 25, 50 µM) for 24 h and subjected to agarose gel electrophoresis followed by ethidium bromide staining. Supercoiled form (top) and open circular form (bottom). Pictures are representative for at least two independent experiments.

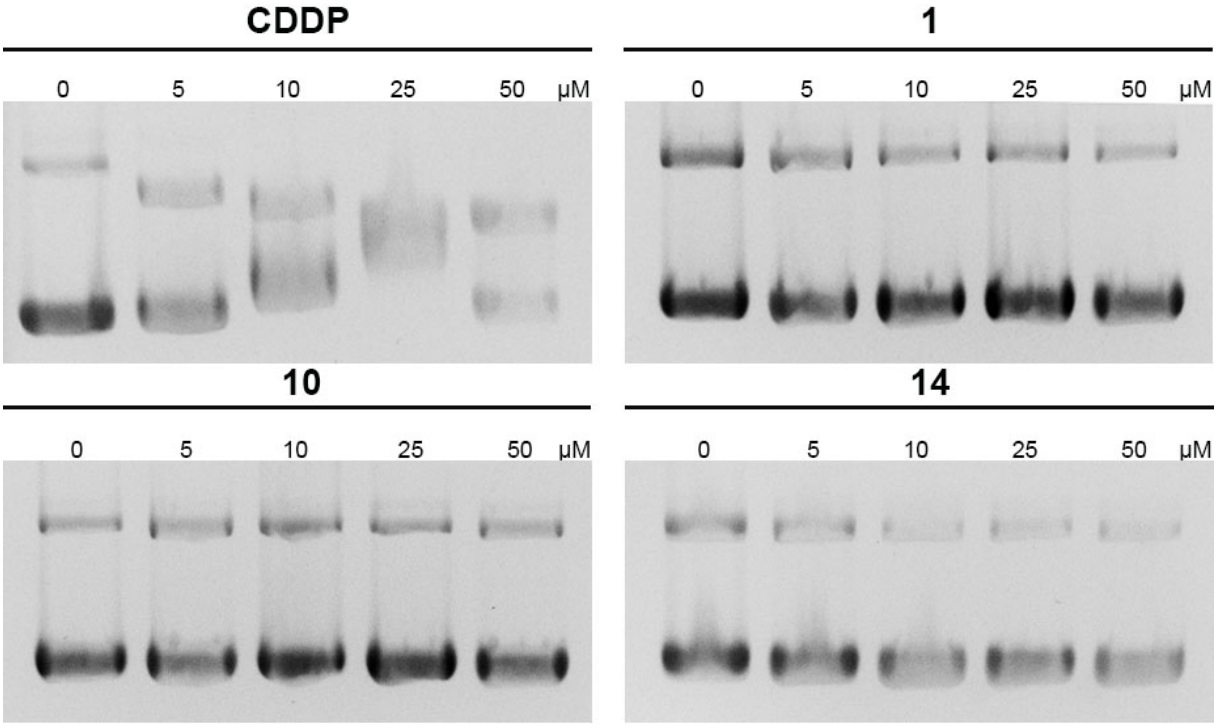

Figure S17. Effect of copper complexes **1–18**, $CuSO_4$, and HL11 on the relative superoxide levels in 518A2 melanoma cells after 24 h incubation as determined by NBT assays. The ROS production (%) was obtained as the mean ± standard deviation of six independent experiments with respect to untreated control cells set to 100 %.

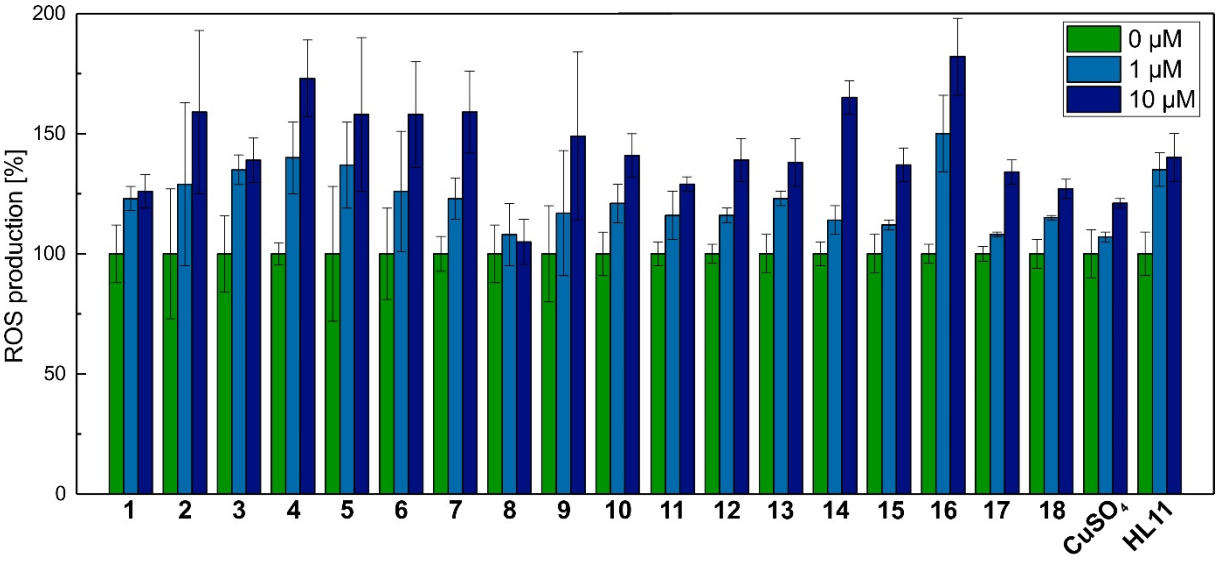

Figure S18. Mass spectrum (DIP, EI, pos.) of **4**.

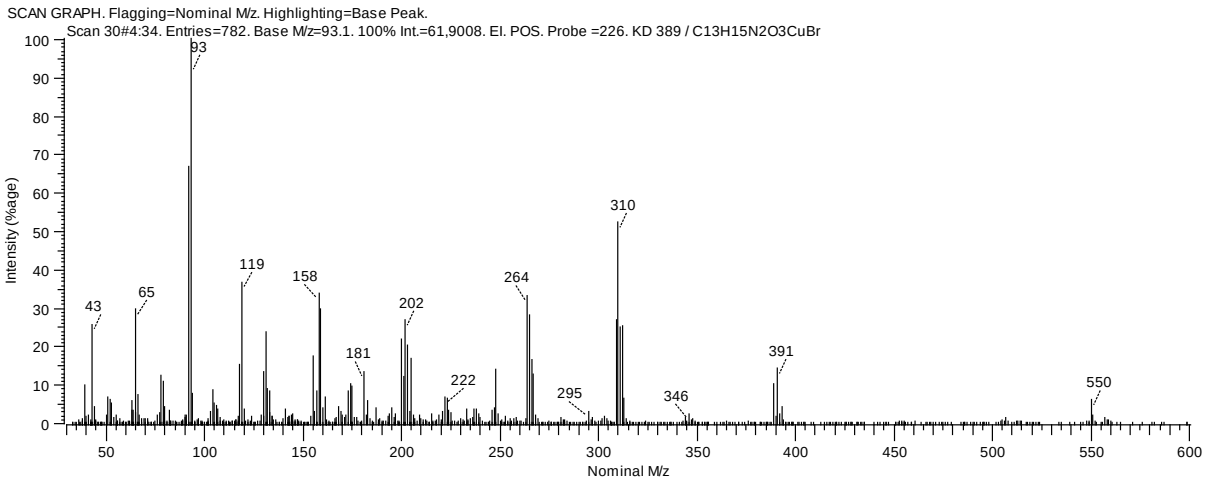

Figure S19. Mass spectrum (DIP, EI, pos.) of **5**.

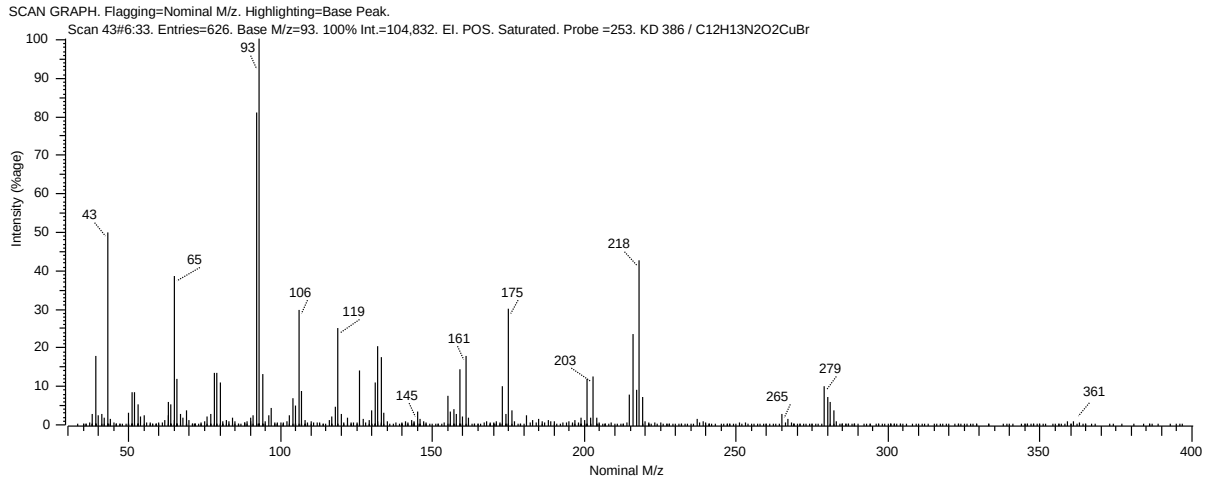

Figure S20. Mass spectrum (DIP, EI, pos.) of **6**.

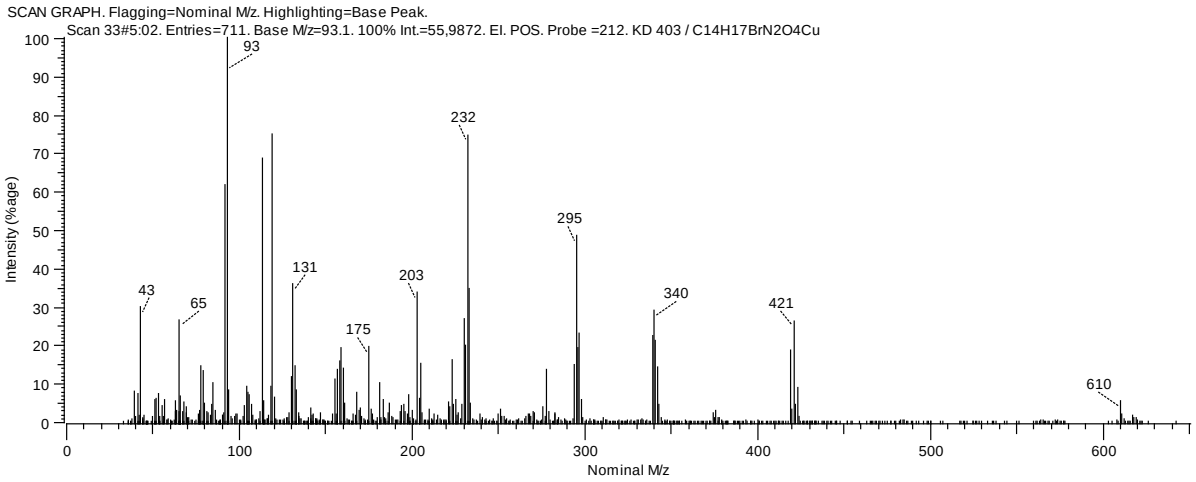

Figure S21. Mass spectrum (DIP, EI, pos.) of **7**.

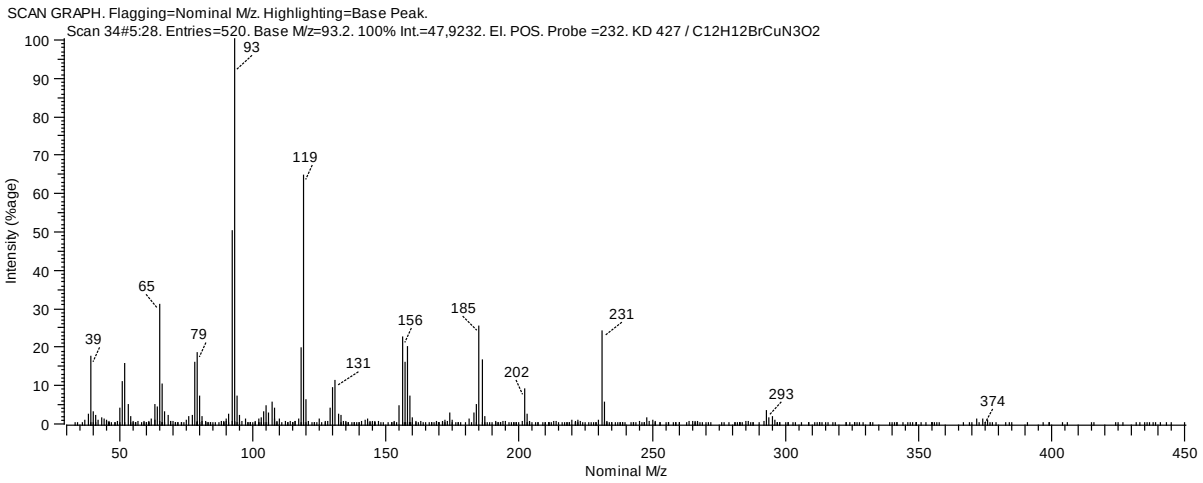

Figure S22. Mass spectrum (DIP, EI, pos.) of **8**.

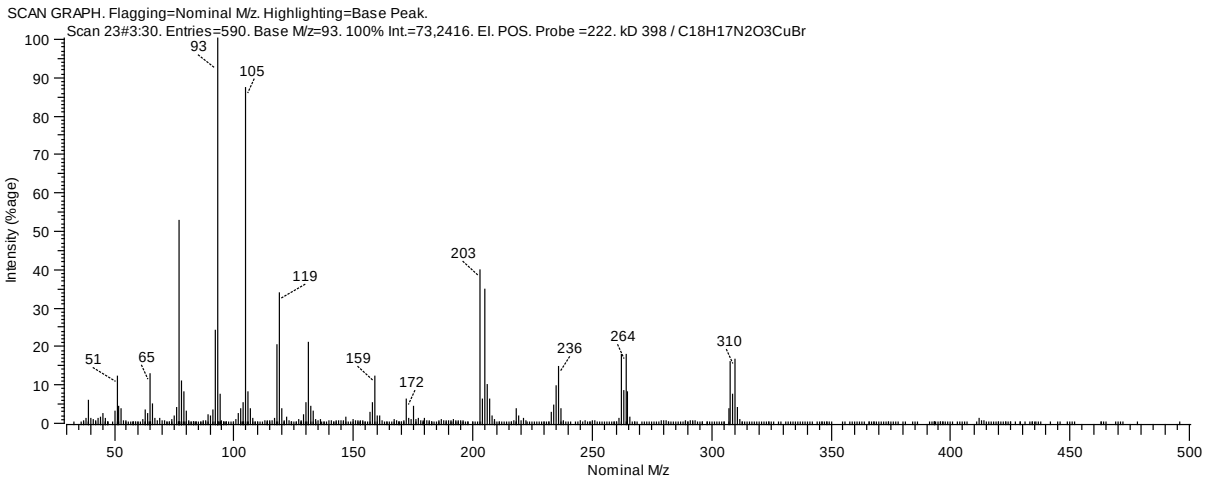

Figure S23. Mass spectrum (DIP, EI, pos.) of **9**.

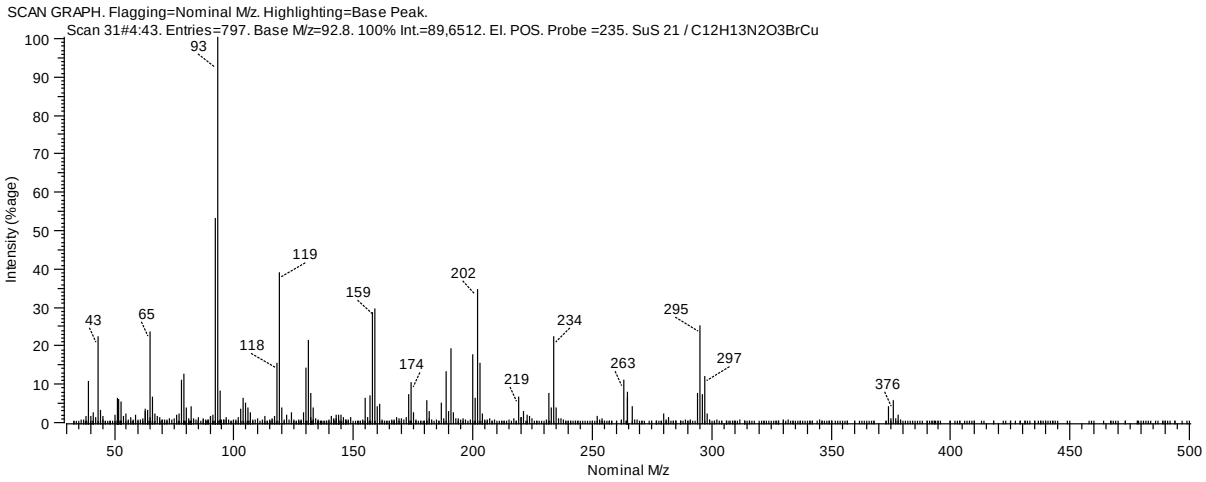

Figure S24. Mass spectrum (DIP, EI, pos.) of **10**.

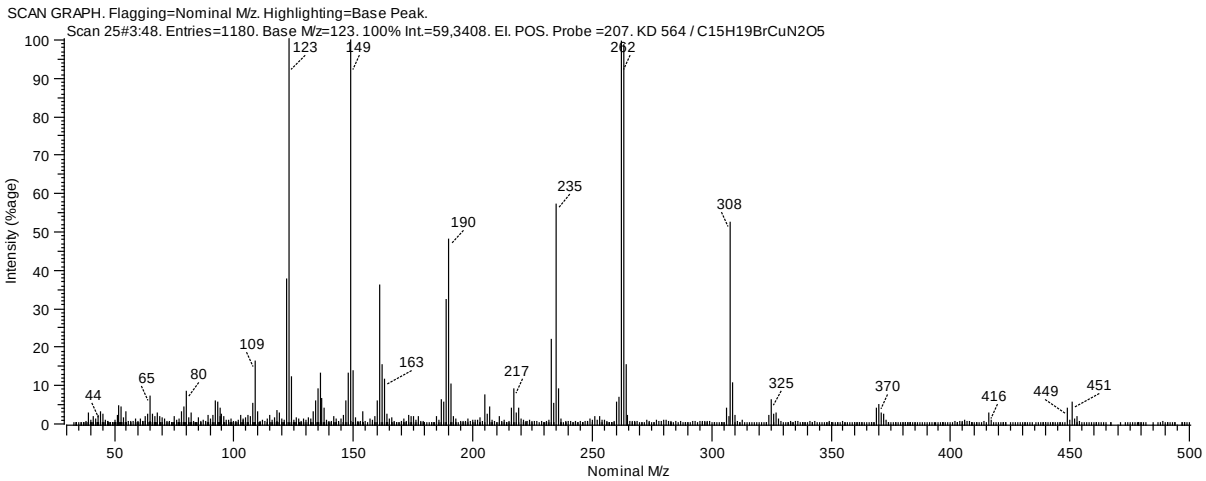

Figure S25. Mass spectrum (DIP, EI, pos.) of **11**.

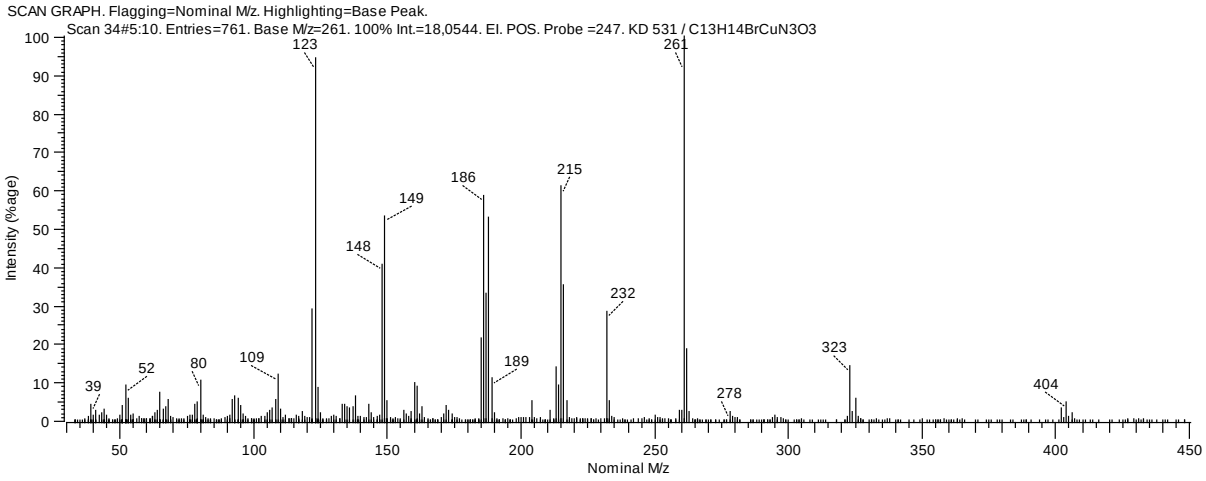

Figure S26. Mass spectrum (DIP, EI, pos.) of **12**.

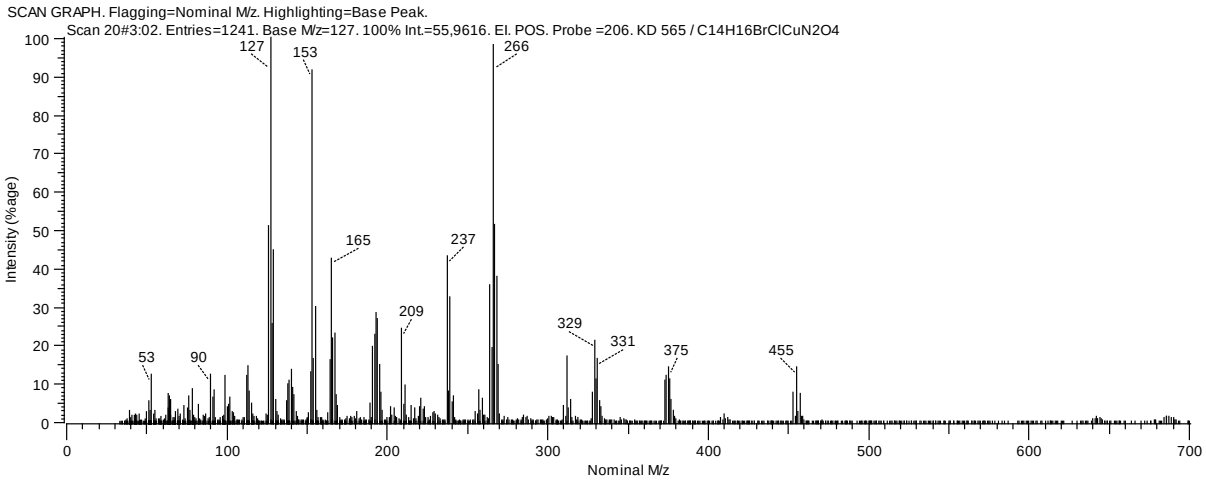

Figure S27. Mass spectrum (DIP, EI, pos.) of **13**.

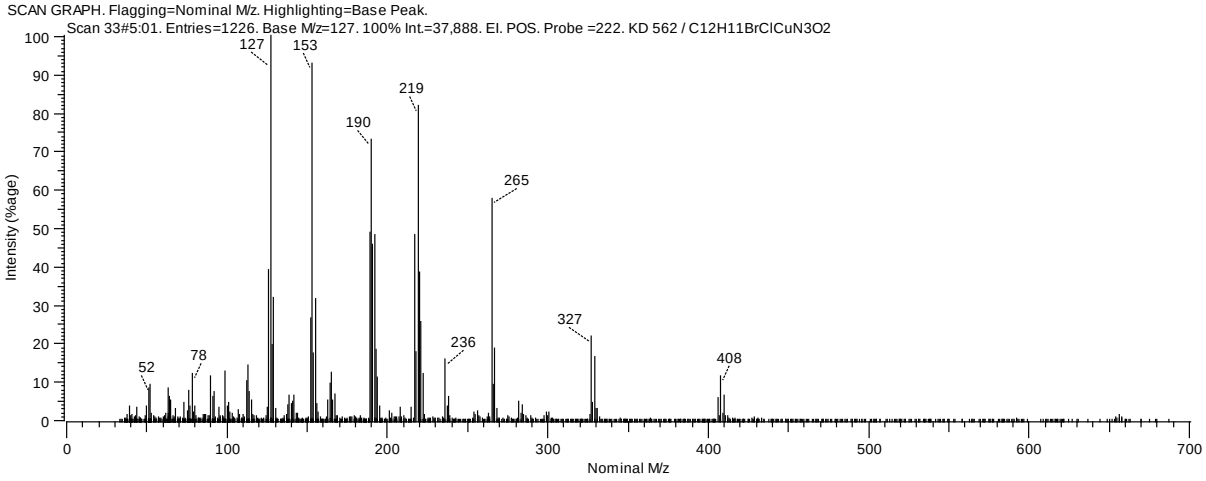

Figure S28. Mass spectrum (DIP, EI, pos.) of **14**.

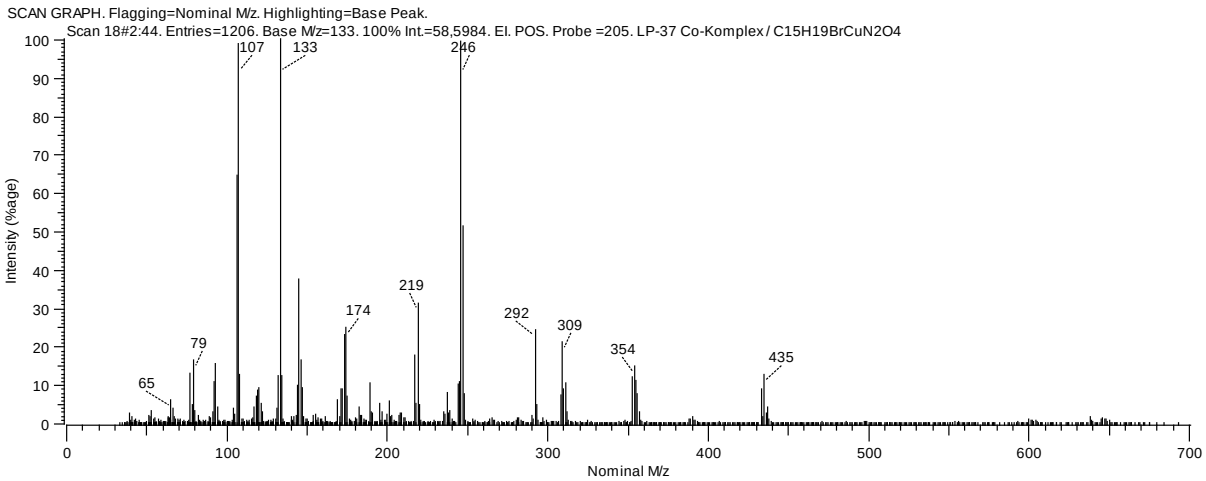

Figure S29. Mass spectrum (DIP, EI, pos.) of **15**.

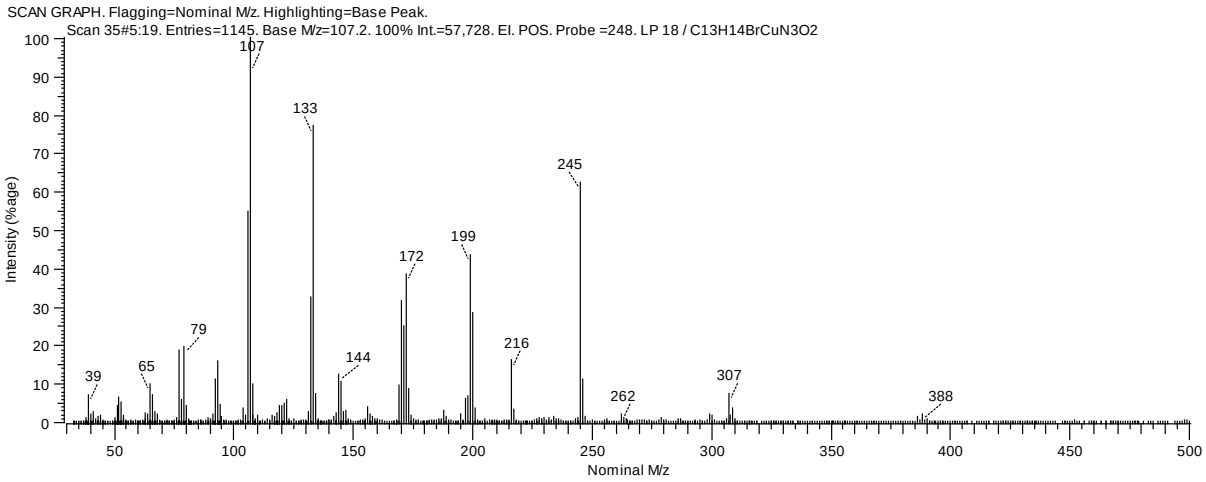

Figure S30. Mass spectrum (DIP, EI, pos.) of **16**.

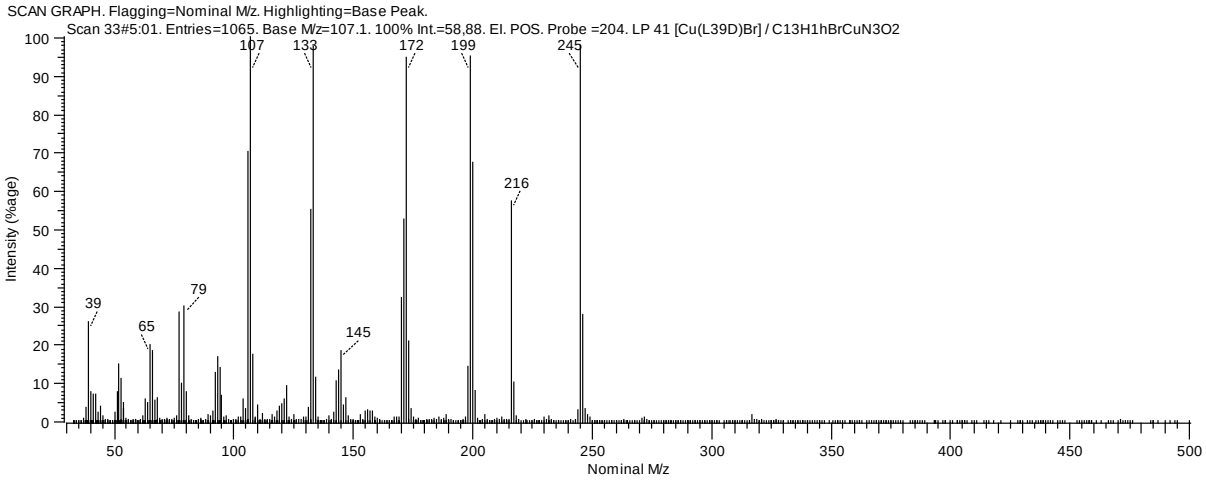

Figure S31. Mass spectrum (DIP, EI, pos.) of **17**.

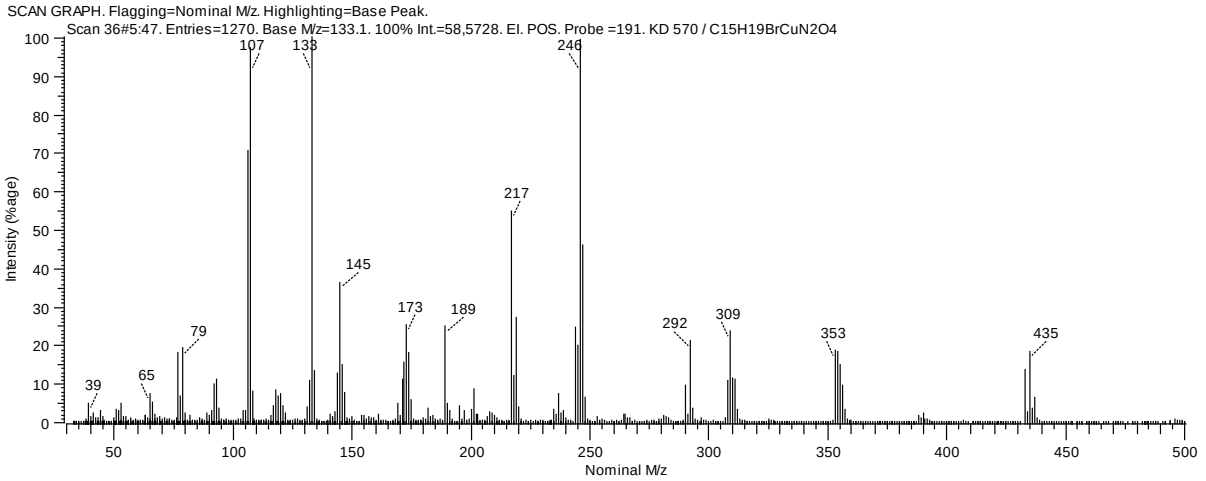

Figure S32. Mass spectrum (DIP, EI, pos.) of **18**.